processes

MDPI

Article

Combustion Efficiency in a Fluidized-Bed Combustor with a Modified Perforated Plate for Air Distribution

Erdiwansyah [1,2,*], Mahidin [3,*], Husni Husin [3], Nasaruddin [4], Muhtadin [5], Muhammad Faisal [5], Asri Gani [3], Usman [5] and Rizalman Mamat [6]

1 Doctoral Program, School of Engineering, Post Graduate Program, Universitas Syiah Kuala, Banda Aceh 23111, Indonesia
2 Faculty of Engineering, Universitas Serambi Mekkah, Banda Aceh 23245, Indonesia
3 Department of Chemical Engineering, Universitas Syiah Kuala, Banda Aceh 23111, Indonesia; husni_husin@unsyiah.ac.id (H.H.); a.gani@unsyiah.ac.id (A.G.)
4 Department of Electrical and Computer Engineering, Universitas Syiah Kuala, Banda Aceh 23111, Indonesia; nasarudin@unsyiah.ac.id
5 Department of Mechanical Engineering, Universitas Abulyatama Aceh, Aceh Besar 23372, Indonesia; muhtadin@gmail.com (M.); m.faisal@gmail.com (M.F.); usman@gmail.com (U.)
6 Faculty of Mechanical Engineering, Universiti Malaysia Pahang, Pekan 26600, Malaysia; rizalman@ump.edu.my
* Correspondence: erdi.wansyah@yahoo.co (E.); mahidin@unsyiah.ac.id (M.); Tel.: +62-81269122570 (M.)

Abstract: Combustion efficiency is one of the most important parameters especially in the fluidized-bed combustor. Investigations into the efficiency of combustion in fluidized-bed combustor fuels using solid biomass waste fuels in recent years are increasingly in demand by researchers around the world. Specifically, this study aims to calculate the combustion efficiency in the fluidized-bed combustor. Combustion efficiency is calculated based on combustion results from the modification of hollow plates in the fluidized-bed combustor. The modified hollow plate aims to control combustion so that the fuel incorporated can burn out and not saturate. The combustion experiments were tested using palm oil biomass solid waste fuels such as palm kernel shell, oil palm midrib, and empty fruit bunches. The results of the measurements showed that the maximum combustion temperature for the palm kernel shell fuel reached 863 °C for M1 and 887 °C for M2. The maximum combustion temperature measurements for M1 and M2 from the oil palm midrib fuel testing reached 898 °C and 858 °C, respectively, while the maximum combustion temperature for M1 and M2 from the empty fruit bunches fuel was 667 °C and M2 847 °C, respectively. The rate of combustion efficiency with the modification of the hole plate in the fluidized-bed combustor reached 96.2%. Thermal efficiency in fluidized-bed combustors for oil palm midrib was 72.62%, for PKS was 70.03%, and for empty fruit bunches was 52.43%. The highest heat transfer rates for the oil palm midrib fuel reached 7792.36 W/m^2, palm kernel shell 7167.38 W/m^2, and empty fruit bunches 5127.83 W/m^2. Thus, the modification of the holed plate in the fluidized-bed combustor chamber showed better performance of the plate than without modification.

Keywords: fluidized-bed combustor; perforated plate; heat transfer; thermal efficiency; combustion efficiency

Citation: Erdiwansyah; Mahidin; Husin, H.; Nasaruddin; Muhtadin; Faisal, M.; Gani, A.; Usman; Mamat, R. Combustion Efficiency in a Fluidized-Bed Combustor with a Modified Perforated Plate for Air Distribution. *Processes* **2021**, *9*, 1489. https://doi.org/10.3390/pr9091489

Academic Editor: Blaž Likozar

Received: 24 July 2021
Accepted: 12 August 2021
Published: 24 August 2021

1. Introduction

Investigations into the efficiency of combustion in FBC fuels using solid biomass waste fuels in recent years are increasingly in demand by researchers around the world. This is due to the existence of highly promising solid biomass wastes that can be converted into energy. Solid biomass waste is one of the renewable energy sources that can be converted to replace fossil energy whose use has been affected and decreased in recent years. The availability of renewable energy is currently abundant in Southeast Asia [1–3]. Abundant renewable energy sources today include a solid waste of palm oil biomass [4–7], where the

results of the analysis with simulations conducted showed that biomass solid waste can produce energy of 106.15 MW from the results of a mixture of several types of biomass, while one type of biomass alone can produce energy of 61.05 MW. Thus, renewable energy sources from palm oil biomass solid waste are suitable for reducing the dependence on fossil fuels, especially in remote areas/islands.

Combustion efficiency is one of the most important parameters especially in the combustion chambers such as the fluidized-bed combustor (FBC). Combustion efficiency, X, can generally be defined as in Equation (1) that shows the definition for combustion efficiency i.e., the ratio of the chemical heat release rate (HRR), Q_{CH}, to the heat of the perfect combustion, Q_T. This is as evidenced in [8].

$$X = \frac{Q_{CH}}{Q_T} \quad (1)$$

An investigation into the efficiency of combustion in the combustion chamber with a case study in a 1:20 scale tunnel has recently been conducted [9], in which the results obtained show that the length of the tunnel can affect the efficiency of combustion. The average value recorded of propane fire reached 89% and for heptane, fire was lower, at 80%. The chemical HRR value decreased from normal fire but the heptane combustion efficiency rate reached 94%. Research to predict the combustion efficiency in methane and propane fires has also been conducted [10], in which the overall combustion efficiency was found to be close to one unit through various oxidizing dilutions, although at the beginning of testing there was a sudden decrease. In different studies conducted with combustion experiments using porous and non-porous alumina base fuel in the FBC, the fuel chamber has been investigated [11], in which the results revealed that polypropylene can be used effectively to fuel both FBC materials. Experiments conducted showed a combustion efficiency rate of 99.9% at 750 °C. Detailed process development to evaluate the heat potential of biomass combustion results in CFB combustion chambers. In addition, research on the analysis of oil palm biomass burning has also been carried out, in which the results of data analysis are obtained through simulations using Aspen Plus and FORTRAN software [12]. An investigation into the efficiency of combustion in FBC fuel using sawdust, rice husks, and cane pulp has been discussed [13]. The experiments tested in the study aimed to investigate temperature, CO, NO, and CO_2 concentrations, in addition to the height of the combustion chamber and the exhaust gases (chimneys). Operating conditions and fuel properties can affect overload and air.

Furthermore, a different study was recently carried out, in which the combustion experiment was conducted using a quatrefoil perforated plate (QPP) [14]. The main purpose of the study was to study the degree of influence of hole height and the QPP plate distance on thermal–hydraulic performance. The results showed that the coefficient of heat transfer and pressure drop on the shell side of the heat exchanger increased with a decrease in hole height and plate distance from the QPP. However, the level of heat transferred on the side of the shell became reduced. Experiments to investigate hydrodynamic loads with two-dimensional perforated plates have been studied [15]. The test results between the two hollow plates with gaps of 0.14 and 0.29 overall showed an excellent association. The topic of modifications of hollow plates in the FBC fuel chamber with the use of biomass solid waste fuel still has very little findings in the literature. The investigation of combustion efficiency in the FBC fuel chamber, especially with palm oil biomass fuel, is also very rarely found in publications. Therefore, research to analyze the efficiency of combustion by making various modifications in the combustion chamber is very important. This is because the use of biomass solid waste as a very abundant source of renewable energy can be used as an alternative fuel to reduce the dependence on fossil energy.

The investigation through experiments conducted in the study specifically aimed to calculate the efficiency of combustion in the FBC combustion chamber. Efficient combustion is calculated based on a modification of the hole plate contained in the FBC combustion chamber. The modified hollow plate aims to control combustion so that the fuel incorpo-

rated can burn out and not saturate. The combustion experiments were tested using palm oil biomass solid waste fuels such as the palm kernel shell (PKS), oil palm midrib (OPM), and empty fruit bunches (EFB).

2. Materials and Experimental Setup

This research was conducted to analyze the level of combustion efficiency through the modification of perforated plates and different fuels. This test was conducted twice for each of the different fuels. The type of fuel and experimental setup designed in the research is described in the stages below.

Material of Fuel

The fuel materials used in the study were solid wastes of palm oil biomass such as the palm kernel shell (PKS), oil palm midrib (OPM), and empty fruit bunches (EFB). Each type of fuel used in this experiment weighed 2.5 kg as shown in Figure 1.

Figure 1. Types of palm oil biomass fuel.

The testing tools used in this experiment include combustion chambers (FBC) and blowers. The designed combustion chamber had an inner circle diameter of 30 cm with a height of 47 cm. Blowers used for wind suppliers into the combustion chamber had a pressure of 14.7 kPa as shown in Figure 2. The temperature measurements and combustion efficiency performed in this experiment were placed at five different points. Measurement was done using the Digital Thermometer HotTemp HT-306 brand. The measurement tool is denoted as M1 (flame temperature), M2 (fire end temperature), M3 (lower freeboard temperature), M4 (upper freeboard temperature), and M5 (outer combustor wall temperature).

The modification of the perforated plates made in this study aimed to analyze the level of breeding efficiency using different fuels. The modification of the perforated plate applied in this study was only the addition of four air suppliers. Thus, the air that enters the combustion chamber can be fulfilled so that the fuel can burn completely and nothing is left. The plate modifications carried out in this test are as shown in Figure 3a. The geometry of the holes drilled in the plate were made based on the previous research conducted by [16]. However, in his research, only hole geometry was carried out. Meanwhile, in this study, the geometry of the existing holes was added with four air guides so that the incoming air supply was sufficient.

Furthermore, the steaming of combustion temperature in this study used the Digital Thermometer HT-306 as shown in Figure 3b and the specifications of the Digital Thermometer HT-306 are presented in Table 1.

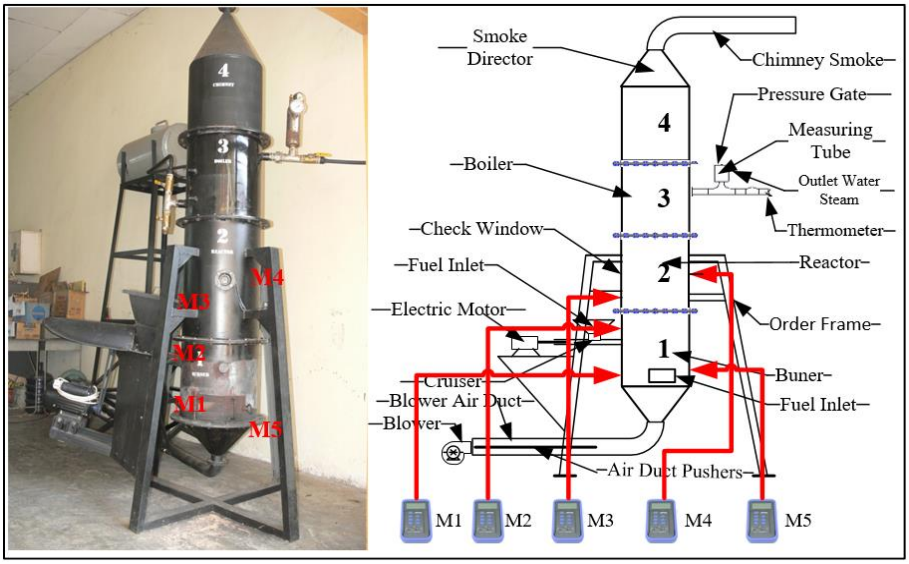

Figure 2. Experimental Setup.

(**a**) (**b**)

Figure 3. (**a**) Modification of hollow plate with four spoons and (**b**) digital thermometer and thermocouple for measurement data.

Table 1. Specifications of the Thermometer Digital HT-306.

Component	Measurement
Model HT-306	Dual channel input
Input sensor	Thermocouple type "K"
Resolution	HT-306:1 °C/1 °F
Response time	15 S
Wide measuring range	−50 °C~+1300 °C (−58 °F~+1999 °F)
Power supply	Baterai 6F22 9V

3. Results and Discussion

3.1. Temperature Influence of Walled Plate Modification

The experiments conducted in this study were tested at five different points with their respective details (M1, M2, M3, M4, and M5). Specifically, the discussion presented in this study concerns the thermal temperature and efficiency of the different fuel test results. Experiments in this study analyzed the level of combustion efficiency in the combustion chamber by modifying the perforated plate with four steering directors in addition to the main steering wheel located in the middle of the plate that has been designed. The results of the combustion temperature analysis measured at the M1 are shown in Figure 4a. The time of the initial combustion to the seventh second indicated that the temperature of the OPF fuel reached 370 °C, which was recorded at the fifth second, while the PKS and EFB fuels showed lower yields. However, at the burning time of 8–16 s, the PKS burn increased to 863 °C, and at 20–30 s, the trend decreased. The resulting maximum temperature of the

OPM fuel iwasrecorded at 21 s, which reached 898 °C. The maximum temperature that fueled the EFB was 667 °C, recorded at 18 s. The low temperature resulting from the OPM combustion due to the higher moisture content was raised by the PKS and EFB.

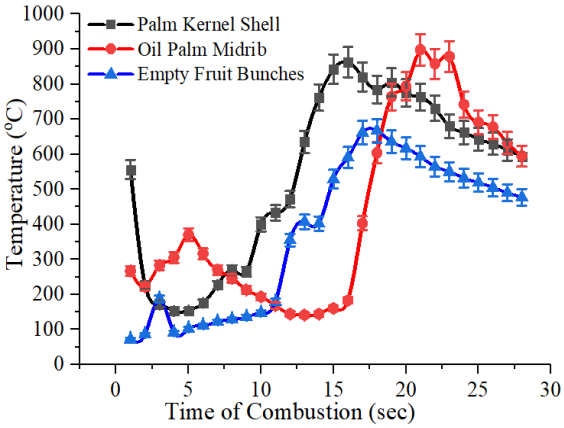

(**a**) Combustion temperature at M1.

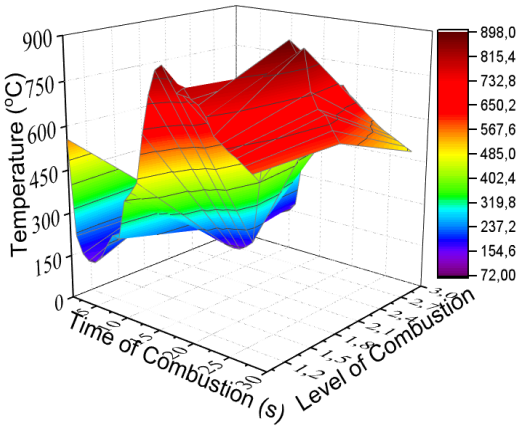

(**b**) Temperature with 3D display.

Figure 4. M1 combustion temperature levels of the three different fuels.

The combustion temperature of the OPM fuel began to increase at seconds 12–18 and continued to decrease until the end of testing. The desperation temperature produced in this study is mainly for the OPM fuel, slightly lower than the results in [17]. However, the amount of fuel in this experiment was less, thus the resulting temperature was lower due to the shorter combustion time. Figure 4b shows the combustion temperature displayed in 3D. It was shown that the combustion temperature of the three fuels used began to increase from 402.4 °C to 815.4 °C and decreased until the end of testing. In addition, the modification of the perforated plate with the four air supplies to the combustion chamber shows that the fuel can burn perfectly compared to the results of previous studies [16].

Temperature measurement results analyzed on M2 with 30 s of three fuel types show that EFB materials are more stable than PKS and OPM as shown in Figure 5a. At the beginning of combustion, OPM fuel showed a significant increase compared to EFB. However, by the time the 11–13 s decreased drastically and began to increase back at 14 s. The maximum combustion temperature of OPM reached 858 °C which was recorded at 20 s and decreased until testing was complete.

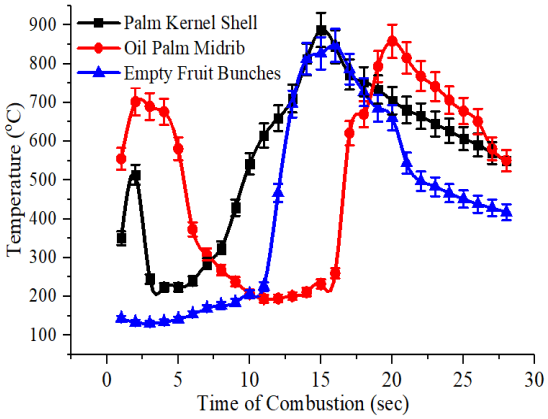

(**a**) Combustion temperature at M2.

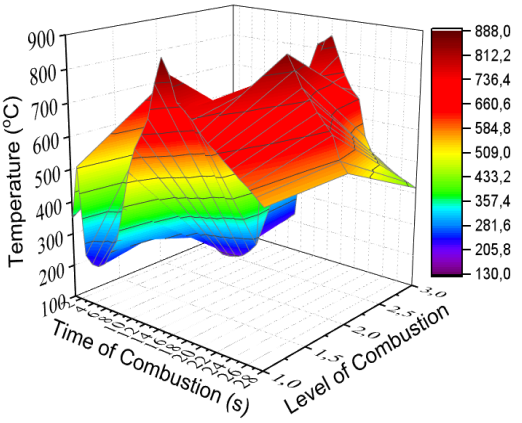

(**b**) 3D display on M2 metering.

Figure 5. Combustion Temperature Level of M2 at Different Time and Fuel.

Test results for PKS fuel analyzed on the M2 showed a slight instability at the start of testing up to 10 s. Furthermore, it continued to increase until the 15th second which reached 887 °C, and decreased until testing was complete. Meanwhile, the combustion temperature from the EFB fuel test results shows a slower trend than PKS and OPM. However, the combustion temperature obtained from burning EFB was lower than that of PKS and OPM. The maximum temperature of EFB fuel test results reached 847 °C as shown in Figure 5a. The combustion fire state of the three types of biomass used is shown in Figure 5b, in which it can be explained that the equalization of fire in the combustion chamber was quite spread out and stable. This is because the wind that enters from the blower through the steering plate of the hole is modified very sufficiently so that the fuel incorporated is burned thoroughly.

Furthermore, the analysis in this test was conducted at the M3 point, which aims to determine the maximum temperature in the lower freeboard chamber after the combustion chamber. The results of the analysis conducted on the M3 reveal that the OPM fuel at the beginning of testing showed a higher temperature than reached 520 °C. This temperature height can be affected by the state of the fire that suddenly rises, resulting in higher temperatures. This is evident clearly at 10 s, decreasing significantly and beginning to increase again at 15 s. The maximum temperature of the analysis using the OPM fuel was recorded at 19 s, reaching 823 °C as shown in Figure 6a. The results of the analysis of the test using the PKS fuel revealed that the maximum combustion temperature reached 870 °C and showed more stable results than the OPM. Meanwhile, the analysis of the EFB fuel usage showed better stability both at the beginning and towards the end of the test. The maximum temperature of the EFB fuel for point M3 reached 747 °C, recorded at 14 s. Temperature stability was analyzed at the M3 test point as shown in Figure 6b, although there was an increase in the initial combustion for the OPM fuel. However, it decreased rapidly to 180 °C and at the 15th second, it started to rise again to 850 °C. The results of combustion are said to be complete when the remaining fuel used can be burned and nothing remains. The remaining fuel from the combustion process tested in the study is shown in Figure 7, in which nothing remains of the rest of the three types of fuel used in this test. Thus, the plate modification designed in this study showed maximum results. This is because the air that enters the combustion chamber is fulfilled by the presence of an excess air supplier.

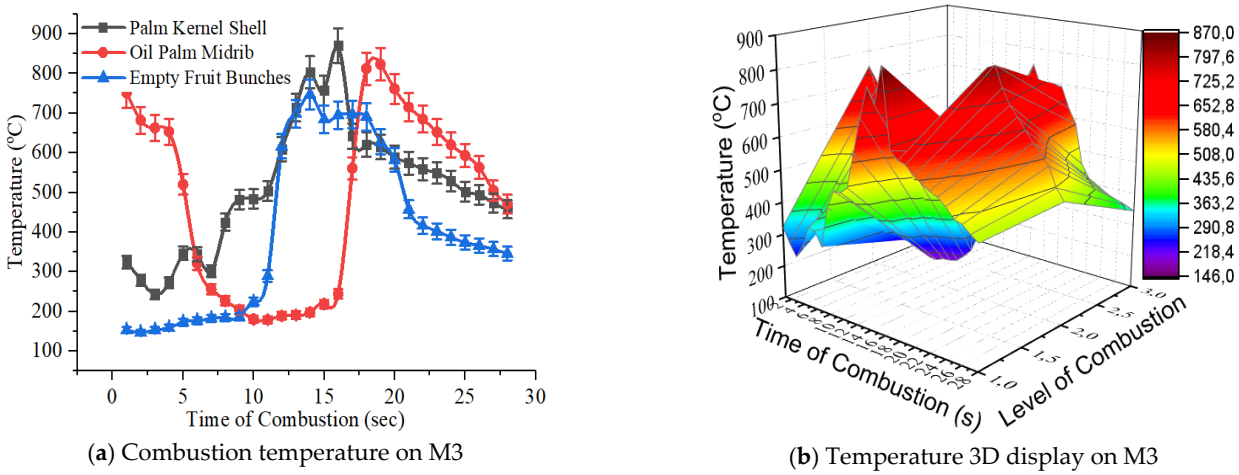

(**a**) Combustion temperature on M3 (**b**) Temperature 3D display on M3

Figure 6. Combustion temperature measurement of M3 at different times and fuels.

Further analysis was conducted in this study at the M4 point with the same time and fuel from the previous analysis. Measurements at the M4 are performed to determine the maximum heat temperature level when reaching the boiler. Based on the results of the analysis, the OPM fuel was slightly higher at 757 °C, recorded at 19 s, while the maximum heat temperature of the PKS and EFB reached 729 °C and 692 °C, respectively, as shown in

Figure 8a. The heat temperature phenomenon of the three types of fuel used shows better results as shown in Figure 8b.

Figure 7. Residual ashes after the burning process.

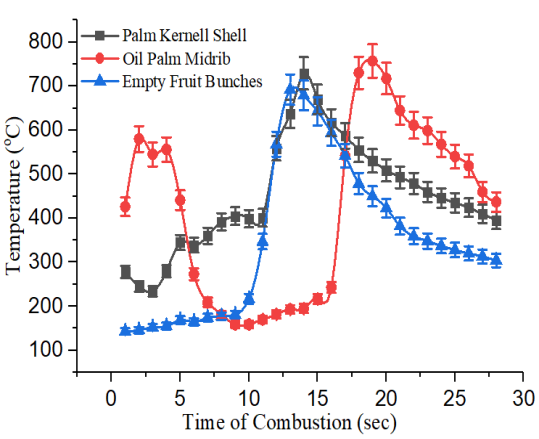

(**a**) Combustion temperature on M4.

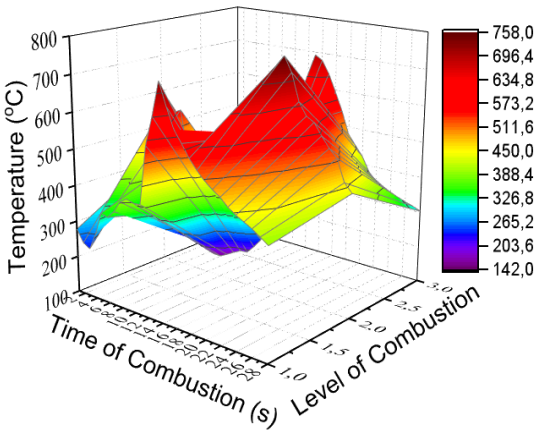

(**b**) 3D temperature display on M4.

Figure 8. Temperature measurement at M4 with different fuels.

The last analysis of the combustion chamber temperature on the outer wall aimed to calculate the level of combustion efficiency. The phenomenon and temperature of the outer combustion chamber walls are necessary to predict the level of efficiency produced. The outer wall temperature of the PKS combustion indicated a stable temperature compared to the OPM and EFB. At 20 s, the temperature shows a drastic decrease in the OPM fuel. This decrease is affected by malfunctioning dredging tools (errors) as shown in Figure 9a. This result is reinforced from the results of the 3D analysis as shown in Figure 9b.

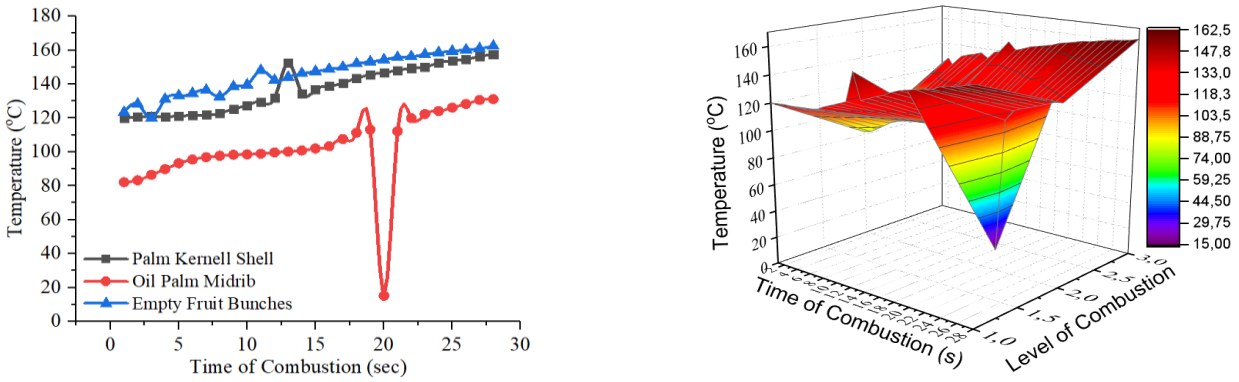

(**a**) Combustion temperature on the outer wall. (**b**) Temperature 3D display on the outer wall.

Figure 9. FBC wall temperature of different fuels.

3.2. Combustion Efficiency

The combustion process in the combustion chamber for producing heating, cooling, and electrical energy needs to be calculated efficiently so that the energy produced can be predicted. The efficiency of the furnace, or better known as the FBC combustion chamber, can be done by Equation (2).

$$\text{Eff} = \frac{P_{out}}{P_{in}} \times 100\% \quad (2)$$

where

Eff is the efficiency,
P_{in} is the power input, and
P_{out} is the power output.

The results of the calculation of the furnace efficiency revealed that the OPM fuels showed better results compared to the PKS and EFB fuels. The furnace efficiency level recorded for OPM was 11.23%, PKS 10.78%, and EFB 9.36% as shown in Figure 10. The results of the search in various publications showed that investigations of the efficiency of fuel furnaces are still very rarely found [18]. Studies comparing thermal efficiency between air–fuel combustion (AFC) and oxy–fuel combustion (OFC) in axial-fueled heating furnaces have been studied [19]. The measurement of the furnace efficiency tested with five different cases can increase efficiency by 50%. However, previous tests have shown that in general efficiency measurements are not within the FBC space. In addition, the fuel used in previous studies was liquid fuel in general.

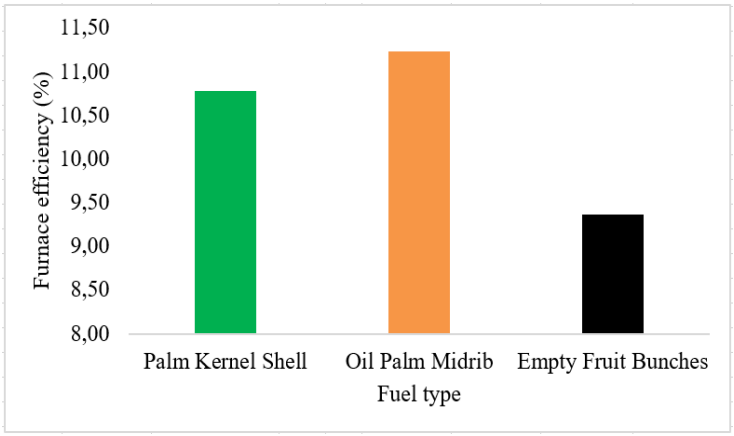

Figure 10. Furnace efficiency in the FBC for different fuels.

3.3. Thermal Efficiency

The calculation of thermal efficiency in a combustion test is a very important variable. It aims to know the efficient combustion resulting from the fuel used. Calculation of thermal efficiency can be done using Equation (3) [20].

$$\eta_{th} = \frac{ma\ Cp\ \Delta T}{mb\ LHV_{fuel}} \quad (3)$$

where

η_{th} is the efficiency thermal,
ma is the liters of water,
Cp is the calorific value,
ΔT is the last value − first value,
mb is the fuel weight, and
LHV_{fuel} is the lower heating value.

Based on the results of the calculations made, thermal efficiency with the use of the OPM fuel reached 72.62%, while the FBC chamber tested using the PKS fuel can produce a thermal efficiency of 70.04% as shown in Figure 11. The EFB fuel combustion testing can deliver thermal efficiency of 52.43%. The level of thermal efficiency in the FBC combustion chamber used in this study was lower than that of [21], in which the final thermal efficiency produced through the design of the solar receiver reached 84.20%. Meanwhile, different studies predicting the thermal efficiency of LPG energy-efficient burners (EB) using CFD data showed lower yields than the thermal efficiency in the FBC space in [22]. The results of the calculation of the experiments conducted from both burners were carried out at 9.02% and 7.87%, respectively. Different studies tested combustion engines using mixed fuels of flaxseed oil and diesel, which showed lower thermal efficiency [23].

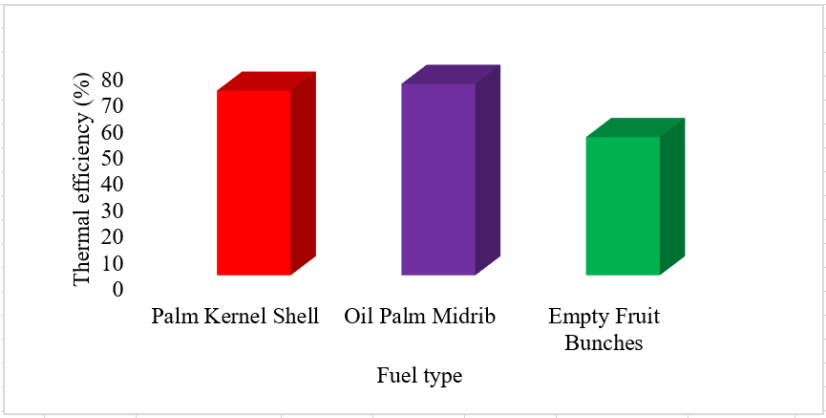

Figure 11. Effect of thermal efficiency for a different fuel.

3.4. Measurement Heat Transfer Coefficient

Calculation of the heat transfer in combustion needs to be done so that the necessary energy can be known. In addition, the calculation of the heat transfer also aims to find out how much efficiency of combustion furnaces is produced in this study. The calculation of the heat transfer in this test was done using Equation (4) [20].

$$q = \frac{M1 - M5}{\frac{1}{hoAo} + \frac{ln\left(\frac{ro1}{ri1}\right)}{k1} + \frac{ln\left(\frac{ro2}{ri2}\right)}{k2} + \frac{ln\ \frac{ro3}{ri3}}{k1} + \frac{1}{hiAi}} \quad (4)$$

where:

q is the convection heat rate;
$M1$ is the temperature fluid;

*M*5 is the temperature wall;
*ro*1 is the outer radius of the cylinder;
*ri*1 is the radius in cylinder;
*ro*2 is the outer radius of insulation;
*ri*2 is the outer radius in isolation;
*ro*3 is the cylinder outer radius;
*ri*3 is the radius in the cylinder;
*k*1 is the thermal conductivity of the plate;
*k*2 is the insulating conductivity;
ho is the convection heat transfer coefficient;
Ao is the outer cross-sectional area;
hi is the coefficient in the wall; and
Ai is the inner cross-sectional area.

Based on the results of the calculations, the rate of heat transfer in the combustion furnaces conducted with the oil palm biomass fuel showed to be higher than the results of experiments in [24]. The heat transfer rate of the OPM fuel reached 7792.36 W/m^2 at 21 min compared to the PKS shown in Figure 12, while the heat transfer rate for EFB fuels showed lower yields of 5127.83 W/m^2 and the PKS of 7167.38 W/m^2. However, the overall fuel used in this study was higher than in [25]. In that study, they used the component of main heat transfer from the fuel combustion, which is primary air, burning as much as 33%, while charcoal did not burn as much as 25%, pots 23%, others by 14%, and fuel space by 6%. The resulting efficiency rate was 24% with a time of 17 min. The experiments conducted in this study used palm oil biomass fuel with a test time of 28 min. Overall, the fuel used was not that important, as shown in Figure 7. The results of the study on the calculation of heat transfer rates conducted earlier are lower than the experiments in [26].

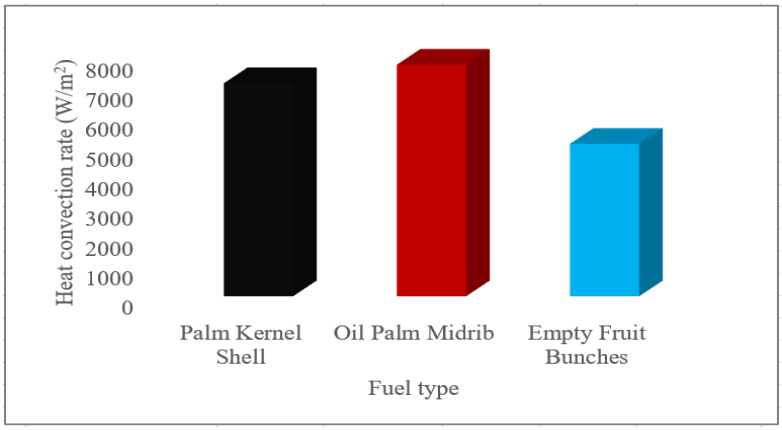

Figure 12. Heat transfer coefficient for a different fuel.

Based on the overall experimental results, the modification of the perforated plate with the addition of four air suppliers shows perfect combustion results because there was no fuel left. At the measurement points M1 and M4, the combustion temperature of the OPM fuel was higher than that of PKS and EFB, as shown in Figures 4 and 8. Meanwhile, the highest combustion temperatures at the M2 and M3 measurement results are recorded from the PKS fuel as shown in Figures 5 and 6. However, the combustion temperature trend shown for EFB fuels shows a slower trend compared to PKS and OPM fuels. The results of combustion using the OPM fuel show a higher combustion efficiency than PKS and EFB. Meanwhile, for thermal efficiency and heat transfer rate, OPM fuel combustion results are also higher than for PKS and EFB. Thus, the modification of the perforated plate with the addition of four air suppliers shows perfect results because there was no fuel left in the combustion chamber. The modification of the hollow plate as we applied in this study is mainly for the burning process of oil palm biomass and, as far as our literature

search confirms, it is the first instance of such a modification. Thus, the application of the modification of the perforated plate in our experiment is the novelty of this work.

4. Conclusions

The tests conducted in the study aimed to analyze the temperature and efficiency of combustion using three different types of biomass fuels. Temperature measurements are allocated at five different points denoted by M1, M2, M3, M4, and M5. The fuel used are palm oil biomass solid wastes such as PKS, OPM, and EFB. The measurement results in this study can draw the following conclusions:

1. Combustion temperatures at M1 and M2 reached 863 °C and 887 °C, respectively, for PKS fuel. The highest combustion temperature recorded at M1 was obtained from OPM fuel at 898 °C. Meanwhile, the highest combustion temperature at M2 was recorded from the combustion of PKS at 863 °C.
2. Modification of the perforated plate with four air suppliers from the blower to the combustion chamber shows maximum results. EFB fuels exhibited a slower combustion temperature trend compared to PKS and OPM fuels.
3. Furnace efficiency levels using PKS, OPM, and EFB fuels were 10.78%, 11.23%, and 9.36%, respectively. Based on these results, it can be reported that OPM fuel shows the maximum combustion furnace efficiency.
4. The highest thermal efficiency in the FBC fuel chamber reached 72.62% for the OPM fuel. Meanwhile, thermal efficiency for the PKS and EFB fuels was 70.03% and 52.43% respectively.
5. The highest heat transfer rate was obtained from OPM fuels reaching 7792.36 W/m^2, while the heat transfer rates for PKS and EFB fuels were 7167.38 W/m^2 and 5127.83 w/m, respectively.
6. Overall, the plate modification applied in this study showed perfect results, indicating that all the fuels used could be burned and nothing remained.

Author Contributions: Conceptualization, E. and M. (Muhtadin); methodology, M.F.; software, U.; validation, A.G.; formal analysis, E.; investigation, R.M.; resources, H.H.; data curation, U.; writing—original draft preparation, E.; writing—review and editing, N.; visualization, H.H.; supervision, M. (Mahidin); project administration, E.; funding acquisition, M. (Mahidin). All authors have read and agreed to the published version of the manuscript.

Funding: This research was funded by Universitas Syiah Kuala, Research institutions, grant number 20/UN11.2.1/PT.01.03/PNBP/2021.

Institutional Review Board Statement: Not applicable.

Informed Consent Statement: Not applicable.

Data Availability Statement: Not applicable.

Acknowledgments: This study was supported by the KEMENRISTEK DIKTI and Higher Education Universitas Syiah Kuala, Research institutions, and community service, with the contract number of 20/UN11.2.1/PT.01.03/PNBP/2021.

Conflicts of Interest: All authors declare that they have no known competing financial interests or personal relationships that could have appeared to influence the work reported in this paper.

References

1. Erdiwansyah; Mamat, R.; Sani, M.S.M.; Sudhakar, K. Renewable energy in Southeast Asia: Policies and recommendations. *Sci. Total Environ.* **2019**, *670*, 1095–1102. [CrossRef]
2. Erdiwansyah; Mahidin; Mamat, R.; Sani, M.S.M.; Khoerunnisa, F.; Kadarohman, A. Target and demand for renewable energy across 10 ASEAN countries by 2040. *Electr. J.* **2019**, *32*, 106670. [CrossRef]
3. Murphy, C.A.; Schleifer, A.; Eurek, K. A taxonomy of systems that combine utility-scale renewable energy and energy storage technologies. *Renew. Sustain. Energy Rev.* **2021**, *139*, 110711. [CrossRef]

4. Shahidul, M.I.; Malcolm, M.L.; Begum, S.; Hashmi, M.S.J.; Islam, M.S.; Eugene, J.J. *Renewable Energy Production From Environmental Hazardous Palm Oil Mill Waste Materials: A Review*; Hashmi, S., Choudhury IABT-E of R and SM, Eds.; Elsevier: Oxford, UK, 2020; pp. 902–914. ISBN 978-0-12-813196-1.
5. Ng, K.H.; Yuan, L.S.; Cheng, C.K.; Chen, K.; Fang, C. TiO_2 and ZnO photocatalytic treatment of palm oil mill effluent (POME) and feasibility of renewable energy generation: A short review. *J. Clean. Prod.* **2019**, *233*, 209–225. [CrossRef]
6. Ahmad, A.; Buang, A.; Bhat, A.H. Renewable and sustainable bioenergy production from microalgal co-cultivation with palm oil mill effluent (POME): A review. *Renew. Sustain. Energy Rev.* **2016**, *65*, 214–234. [CrossRef]
7. Mahidin; Saifullah; Erdiwansyah; Hamdani; Hisbullah; Hayati, A.P.; Zhafran, M.; Sidiq, M.A.; Rinaldi, A.; Fitria, B.; et al. Analysis of power from palm oil solid waste for biomass power plants: A case study in Aceh Province. *Chemosphere* **2020**, *253*, 126714. [CrossRef]
8. Tewarson, A. Generation of heat and chemical compounds in fires. *SFPE Handb. Fire Prot. Eng.* **2002**, 82–161. Available online: https://www.semanticscholar.org/paper/Generation-of-Heat-and-Chemical-Compounds-in-Fires-Tewarson/845faf6dc5e9d9bc6da273f5b21078b62df83a1a (accessed on 11 August 2021).
9. Ishikawa, T.; Kasumi, K.; Tanaka, F.; Moinuddin, K.A.M. Combustion efficiency during fires in tunnels with natural ventilation by vitiated air including descending smoke. *Fire Saf. J.* **2020**, *120*, 103093. [CrossRef]
10. White, J.P.; Link, E.D.; Trouvé, A.; Sunderland, P.B.; Marshall, A.W. A general calorimetry framework for measurement of combustion efficiency in a suppressed turbulent line fire. *Fire Saf. J.* **2017**, *92*, 164–176. [CrossRef]
11. Qin, L.; Han, J.; Chen, W.; Yao, X.; Tadaaki, S.; Kim, H. Enhanced combustion efficiency and reduced pollutant emission in a fluidized bed combustor by using porous alumina bed materials. *Appl. Therm. Eng.* **2016**, *94*, 813–818. [CrossRef]
12. Peng, W.; Liu, Z.; Motahari-Nezhad, M.; Banisaeed, M.; Shahraki, S.; Beheshti, M. A detailed study of oxy-fuel combustion of biomass in a circulating fluidized bed (CFB) combustor: Evaluation of catalytic performance of metal nanoparticles (Al, Ni) for combustion efficiency improvement. *Energy* **2016**, *109*, 1139–1147. [CrossRef]
13. Permchart, W.; Kouprianov, V.I. Emission performance and combustion efficiency of a conical fluidized-bed combustor firing various biomass fuels. *Bioresour. Technol.* **2004**, *92*, 83–91. [CrossRef]
14. Wang, D.; Wang, H.; Xing, J.; Wang, Y. Investigation of the thermal-hydraulic characteristics in the shell side of heat exchanger with quatrefoil perforated plate. *Int. J. Therm. Sci.* **2021**, *159*, 106580. [CrossRef]
15. Mentzoni, F.; Kristiansen, T. Two-dimensional experimental and numerical investigations of parallel perforated plates in oscillating and orbital flows. *Appl. Ocean Res.* **2020**, *97*, 102042. [CrossRef]
16. Hani, M.R.; Mahidin, M.; Husin, H.; Khairil, K.; Hamdani, H.; Erdiwansyah, E.; Hisbullah, H.; Faisal, M.; Mahyudin, M.; Muhtadin, M. Experimental Studies on Combustion Characteristics of OilPalm Biomass in Fluidized-Bed: A Heat Energy Alternative. *J. Adv. Res. Fluid Mech. Therm. Sci.* **2020**, *68*, 9–28. [CrossRef]
17. Ninduangdee, P.; Kuprianov, V.I. Combustion of Oil Palm Shells in a Fluidized-bed Combustor Using Dolomite as the Bed Material to Prevent Bed Agglomeration. *Energy Procedia* **2014**, *52*, 399–409. [CrossRef]
18. Liu, Y.; Wang, J.; Min, C.; Xie, G.; Sundén, B. Performance of fuel-air combustion in a reheating furnace at different flowrate and inlet conditions. *Energy* **2020**, *206*, 118206. [CrossRef]
19. Han, S.H.; Lee, Y.S.; Cho, J.R.; Lee, K.H. Efficiency analysis of air-fuel and oxy-fuel combustion in a reheating furnace. *Int. J. Heat Mass Transf.* **2018**, *121*, 1364–1370. [CrossRef]
20. Holman, J.P. Perpindahan Kalor (terjemahan E. Jasfi). *Jkt. Penerbit Erlangga (Buku Asli 1986)*. 1988. Available online: https://onesearch.id/Record/IOS2862.UNMAL000000000013905 (accessed on 11 August 2021).
21. Xiao, G.; Zeng, J.; Nie, J. A practical method to evaluate the thermal efficiency of solar molten salt receivers. *Appl. Therm. Eng.* **2021**, *190*, 116787. [CrossRef]
22. Wichangarm, M.; Matthujak, A.; Sriveerakul, T.; Sucharitpwatskul, S.; Phongthanapanich, S. Investigation on thermal efficiency of LPG cooking burner using computational fluid dynamics. *Energy* **2020**, *203*, 117849. [CrossRef]
23. Agrawal, B.N.; Sinha, S.; Kuzmin, A.V.; Pinchuk, V.A. Effect of vegetable oil share on combustion characteristics and thermal efficiency of diesel engine fueled with different blends. *Therm. Sci. Eng. Prog.* **2019**, *14*, 100404. [CrossRef]
24. Yu, Z.; Tao, L.; Huang, L.; Wang, D. Numerical investigation on cooling heat transfer and flow characteristic of supercritical CO_2 in spirally fluted tubes. *Int. J. Heat Mass Transf.* **2020**, *163*, 120399. [CrossRef]
25. Gogoi, B.; Baruah, D.C. Steady state heat transfer modeling of solid fuel biomass stove: Part 1. *Energy* **2016**, *97*, 283–295. [CrossRef]
26. Faisal, M.; Usman, U. Analisa Perpindahan Panas Pada Tungku Rocket Tipe Silinder Berbahan Bakar Biomassa. In Proceedings of the Prosiding SEMDI-UNAYA (Seminar Nasional Multi Disiplin Ilmu UNAYA), Banda Aceh, Indonesia, 20–21 June 2019; Volume 3, pp. 393–401.